EUROPEAN ORGANIZATION FOR NUCLEAR RESEARCH

/afm CERN/PS/89-04 (AR)

PINCH CURRENT ENHANCEMENT BY THE INVERSE SKIN EFFECT

E. Boggasch*, J. Christiansen, K. Frank, R. Tkotz
Physikalisches Institut der Universität Erlangen-Nürnberg
D-8520 Erlangen

and

H. Riege
CERN, CH-1211 Geneva 23

Abstract

The dynamics of a linear z-pinch discharge are studied. The magnetic field distribution inside the discharge tube was measured by small magnetic probes. It was found that the "inverse skin effect" which occurs after the maximum contraction of the plasma column causes a strong pinch current enhancement. This observation favours the use of a z-pinch discharge as a focusing device ("plasma lens") for high-energy particles as it is foreseen for the CERN ACOL (Antiproton Collector) project.

Paper submitted for publication in Plasma Physics and Controlled Fusion

Geneva, Switzerland
January 1989

---

* Present address: Laboratory for Plasma Research, Univ. of Maryland, College Park, MD 20742, USA.

1. INTRODUCTION

The azimuthal magnetic field of a linear high-current z-pinch discharge can be used to focus diverging high-energy charged particles as successfully demonstrated in 1965 at the Brookhaven National Laboratory (Forsyth et al., 1965). If constant current density is achieved in a cylindrically symmetric, pinched plasma column, it can be used as a strong constant-gradient magnetic lens ("plasma lens"). For the ACOL-project at CERN, such a powerful lens is necessary to focus antiprotons leaving the production target within a wide cone (Autin et al., 1987). It has been under consideration for some time to install such a plasma lens in the ACOL target area to significantly increase the amount of captured antiprotons.

In 1983 a plasma lens development program was set up at CERN and a variety of z-pinch discharge systems were studied in the required parameter region (See Table I) (Dothan et al., 1987; Boggasch, 1987).

Table I - Parameter values for an ACOL plasma lens

Length	300 mm
Diameter	40 mm
Current	400 kA
Magnetic field at radius 20 mm	4 T
Duration of field	500 ns
Repetition rate	2.4 s
Lifetime	>1.5 10^6 discharges

Magnetic field measurements inside the discharge tube were used to study the plasma dynamics under different discharge conditions such as charging voltage, gas type, pressure, and wall material.

The results showed strong surface currents, which were re-initiated near the wall during the discharge, especially in heavy gases, thus lowering the field amplitude in the center region (Autin et al., 1987). These negative effects could be drastically reduced by using hydrogen as the discharge gas together with thermo-shock resistant ceramic wall materials.

The experiments also showed a favorable current and field enhancement effect in the center plasma column caused by the "inverse skin effect". This effect was previously mentioned by Haines (1959) as a mechanism eventually to be observed during a pinch discharge.

Closed current loops, independent of the external circuit current, were observed inside the plasma. For the first time quantitative experimental data on the dynamics of this effect will be presented. A simple condition can be derived to predict the observed phenomena.

The general appearance of the inverse skin effect in a wide range of discharge parameters hints to its importance also in other types of high current discharges.

2. *EARLIER INVESTIGATIONS OF THE INVERSE SKIN EFFECT*

The dynamic z-pinch discharge was regarded in the early 1950's as a possible candidate for achieving controlled nuclear fusion conditions, and therefore it was the subject of many experiments.

Burkhardt and Lovberg (1958) reported about a "self-trapping of currents" in a stabilized z-pinch discharge due to the "negative skin effect". They assumed as a necessary condition for the appearance of this effect that the discharge period had to be greater than the diffusion time of the outside magnetic field into the plasma region.

Haines (1959) developed a general theory of the inverse skin effect. He calculated the axial current distribution of a rigid cylindrical conductor and derived quantitative results. He showed that the gradient of the current density dj_z/dr at the surface of the conductor with radius $r = a$ is proportional to the time-derivative dI_z/dt of the total current through the conductor:

$$\left(\frac{dj_z}{dr}\right)_{r=a} = \frac{\mu_0 \sigma}{2\pi a} \cdot \frac{dI_z}{dt} \quad , \tag{1}$$

where μ_0 is the vacuum permeability and σ the conductivity. It can be seen from Eq. (1) that negative current flow at the conductor surface can only be produced by a negative dI_z/dt. He pointed out that by this onset

of negative currents instabilities could be induced when the conductor is a plasma.

I.F. Kvartshkhava et al. (1971) observed a "coaxial stratification" of the pinched plasma column by means of fast photographic methods and considered this due to the influence of the inverse skin effect. However, little quantitative experimental evidence was given about the current distribution inside the discharge chamber.

Jones and Silawatshananai (1980) presented data which they considered to be an "unambiguous observation of the reversed current effect" in a z-pinch discharge of 30 kA, stabilized by an axial magnetic field. The temporal behavior of this process, however, was evaluated again only by photographic methods.

In this paper we will present quantitative data of the whole dynamic pinching process, including the formation of a negative current sheath and its ejection towards the outer wall.

3. EXPERIMENTAL OBSERVATIONS

The experiments were performed with a specially designed pulse generator which delivered current pulses of 500 kA to a centrally located z-pinch plasma lens (Boggasch et al., 1985). Four capacitor banks of 27 μF charged up to 20 kV were switched simultaneously by four high-current pseudospark switches (Bloess et al., 1983; Billault et al., 1987). The current in each of the transfer strip lines, as well as the total current through the z-pinch tube, was monitored by specially built Rogowski coils as described by Boggasch and Grüb (1986).

For the experiments reported in this paper alumina or quartz tubes were used. They had a length of 250 mm and diameters between 204 mm and 240 mm.

Two small inductive probes were inserted at certain longitudinal positions from opposite sides into the discharge tube to measure the azimuthal magnetic field $B_\varphi(r,t)$ at different radii as a function of time (Fig. 1).

A probe consisted of a miniature coil of 40 turns and 0.75 mm diameter and was partly shielded in the usual way as described by Böttticher

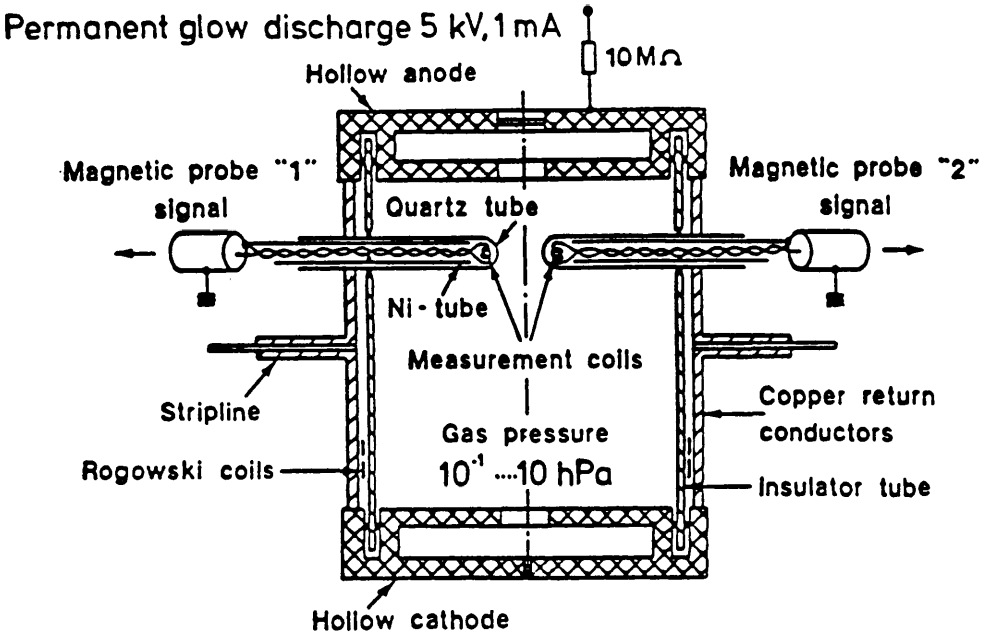

Fig. 1 - Schematic of the magnetic field measurement set-up. Note that probes are drawn in a scale which is large as compared to the discharge tube.

(1968). For the given parameter range, their inductance was low enough to achieve a sufficiently small rise time in a 50 Ω circuit (8 ns). The quartz tubes, insulating and protecting the probes from the plasma, had an outer diameter of 4 mm, which was small enough to keep the perturbation of the plasma negligible.

During one measuring series, both probes were moved from shot to shot in small steps of a few millimeters to obtain data across the whole tube diameter. The probe signals were recorded and numerically evaluated. By comparing the data of both probes, discharge symmetry could be checked. Successive shots under the same conditions allowed verification of the discharge reproducibility necessary for the data treatment.

After evaluating the azimuthal magnetic field $B_\vartheta(r_i,t)$ the time-dependent current $\delta I_z(r_i/r_t,t)$ in a cylindrical shell between two neighbouring radii r_i and r_k (assuming cylindrical symmetry) was found as

$$\delta I_z(r_i/r_k,t) = 2\pi/\mu_0[r_k B_\vartheta(r_k,t) - r_i B_\vartheta(r_i,t)]$$

When plotting δI_z as a function of time for different radial shells, a clear image of the current flow inside the tube is established. This diagram is generally more informative than a current density diagram.

4. RESULTS

A typical current distribution evaluated according to Eq. (2) is shown in Fig. 2a. The current flow starts at the outer shell and penetrates to smaller radii with increasing time. By summation of all curves in Fig. 2a the total current can be obtained, as it is measured by the external Rogowski coil. Two μs after ignition, a current flow near the wall starts a second time. At pinch time t_p the current peaks inside a radius of 10 mm, as can be seen in Fig. 2b. Between t_p and t_{imax}, a strong rise in current near the axis up to about 30 mm -and a simultaneously occurring strong negative current between 30 and 60 mm- is measured. The current near the axis at time txmax is almost doubled compared to time t_p. Within 300 ns the negative current shell moves towards the outer wall and causes a sharp decay of the current within a 90 to 100 mm radius near the insulator wall. This current enhancement effect could be observed over a whole parameter range, and could even cause the pinch

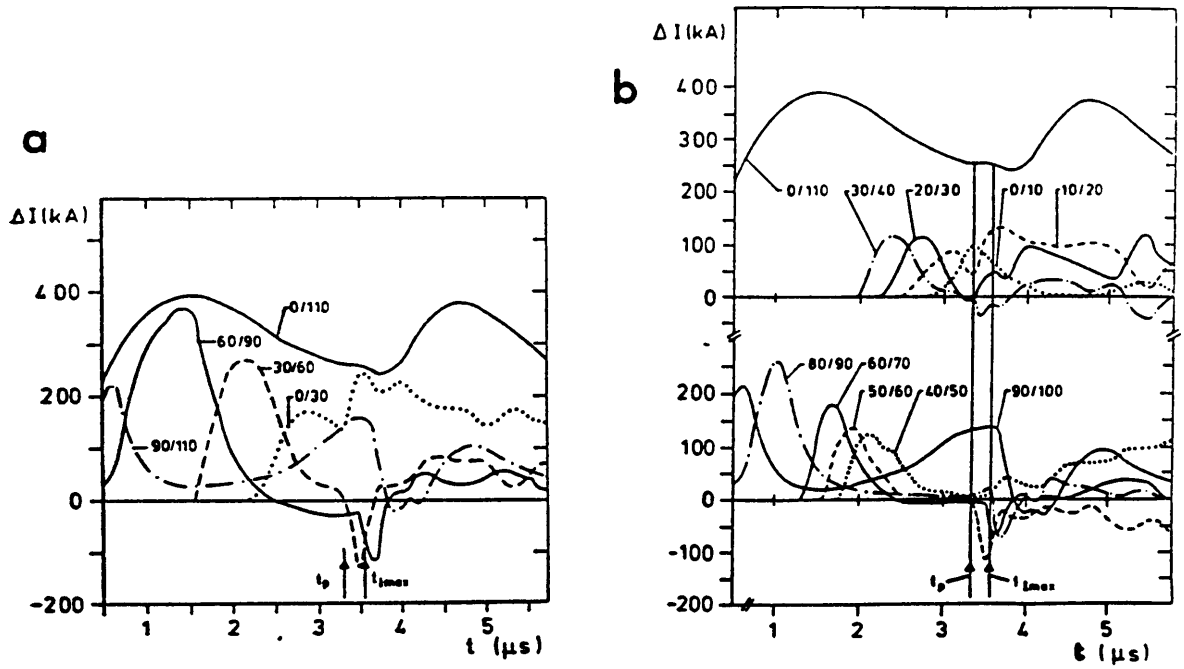

Fig. 2 - Current distribution inside the discharge tube (alumina) filled with hydrogen at a pressure of 400 Pa. The charging voltage was 15 kV. The number of each curve indicates the radial boundaries in mm.

a) Overall distribution. Note the onset of strong negative currents at pinch time t_p between 30 and 60 mm, and a simultaneous positive enhancement between 0 and 30 mm.

b) Same as a), but with smaller shell subdivision (higher spatial resolution.

current to exceed the actual total current in the outer circuit as is seen in Fig. 3.

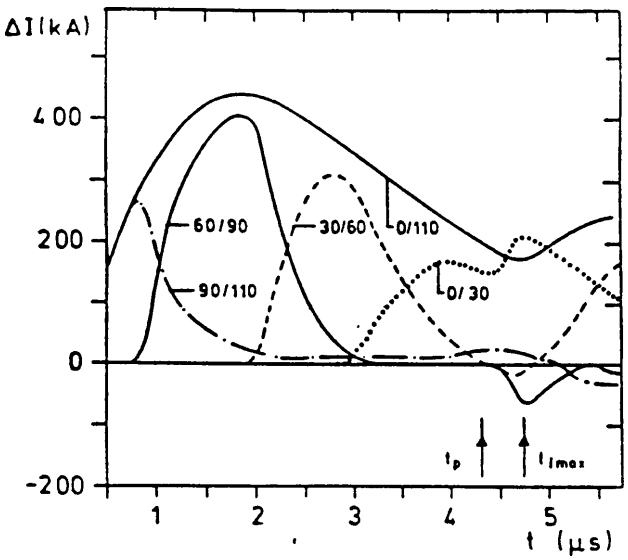

Fig. 3

Current distribution for a 15 kV charging voltage and hydrogen gas at 800 Pa. The current amplification within a 300 mm radius at time t_{imax} exceeds the actual total current by about 300 kA.

In the example of Fig. 4, the maximum contraction of the pinch occurs when the total current is almost zero. This experiment was performed in a quartz tube which was protected against plasma radiation by a number of separated copper rings fixed to the inner tube surface (Boggasch, 1987). Also, in this case the enhancement effect initiates a positive current flow of 135 kA within a 20 mm radius when the total current passes the zero line. The formation and the outward movement of the negative current layer occurs rather slowly and can be clearly observed.

5. *DISCUSSION*

The current enhancement seems to be a generally observable phenomenon existing in at least the parameter range covered by the experiments. It can be explained by the inverse skin effect. It was possible to measure the entire dynamics of this process in a simple unstabilized pinch discharge. The effect was always observed when the pinched column started to expand. A condition for the appearance of the inverse skin effect will now be derived.

The discharge scheme of the pinched plasma column is shown in Fig. 5. The plasma radius r_p is a function of time, whereas radii r_i and r_a are considered fixed in space. Assuming constant current density within

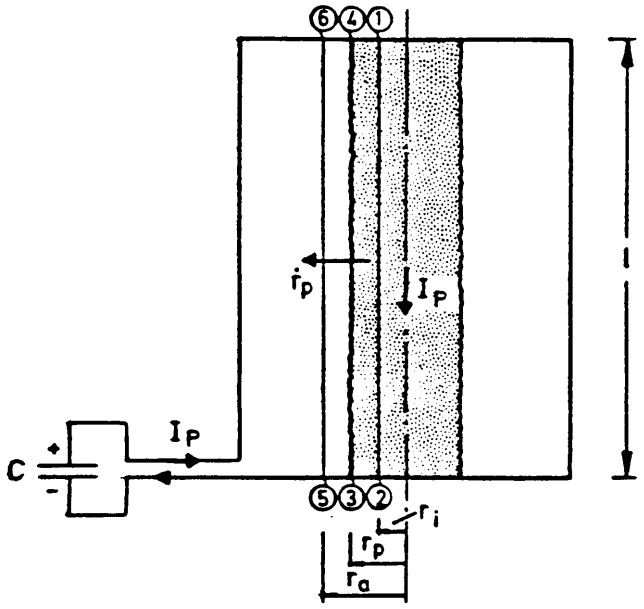

Fig. 5

Current distribution for a 10 kV charging voltage and helium gas at 260 Pa. In this case the inner surface of the quartz discharge tube was partly screened by 20 separate copper rings. The outward velocity of the negative current layer is 3.15 cm/μs.

the plasma column, the magnetic flux Φ_i through the area encircled by the curve 1-2-3-4-1 is calculated as

$$\Phi_i = \int_{r_i}^{r_p} \frac{\mu_0 I_p r'}{2 r_p^2 \pi} \, dr' = \frac{\mu_0 I_p l}{4\pi} \left(1 - \frac{r_i^2}{r_p^2}\right). \tag{3}$$

The flux Φ_a through an area outside, encircled by the curve 4-3-5-6-4, is

$$\Phi_a = \int_{r_p}^{r_a} \frac{\mu_0 I_p l}{2\pi r'} \, dr' = \frac{\mu_0 I_p l}{2\pi} \ln \frac{r_a}{r_p} \, . \tag{4}$$

Owing to Faraday's law, the negative time derivative of the magnetic flux induces an electric field along the encirculating curves:

$$\int_{1\text{-}2\text{-}3\text{-}4\text{-}1} \underline{E} \cdot d\underline{s} = -\frac{d}{dt} \Phi_i = -\frac{\mu_0 l}{2\pi} \left[\frac{\dot{I}_p}{2} \left(1 - \frac{r_i^2}{r_p^2}\right) + I_p \frac{r_i^2}{r_p^3} \dot{r}_p \right] \tag{5}$$

$$\int_{1\text{-}2\text{-}5\text{-}6\text{-}1} \underline{E} \cdot d\underline{s} = -\frac{d}{dt} \Phi_a = -\frac{\mu_0 l}{2\pi} \left(I_p \ln \frac{r_a}{r_p} - I_p \frac{\dot{r}_p}{r_p} \right) \tag{6}$$

Summation of both integrals yield

$$\int_{1\text{-}2\text{-}5\text{-}6\text{-}1} \underline{E} \cdot d\underline{s} = \frac{\mu_0 l}{2\pi}\left[\left(1 - \frac{r_i^2}{r_p^2}\right)\left(-\frac{\dot{I}_p}{2} + \frac{I_p \dot{r}_p}{r_p}\right) - \dot{I}_p \ln\frac{r_a}{r_p}\right] \qquad (7)$$

The integral is positive under the condition

$$\left(1 - \frac{r_i^2}{r_p^2}\right)\left(-\frac{\dot{I}_p}{2} + \frac{I_p \dot{r}_p}{r_p}\right) > \dot{I}_p \ln\frac{r_a}{r_p} \qquad (8)$$

A positive voltage is induced along the path 1-2-5-6-1 which can give rise to a circulating current flow.

The left-hand term gives values between 0 and 1 depending on the ratio r_i/r_p, which determines the inner radius of current enhancement:

$r_i = r_p$ The induced current flows on the plasma surface. Here condition (8) can only be fulfilled for negative dI_p/dt values, in agreement with Haine's case of a metallic conductor in equation (1).

$r_i = 0$ The current is induced on the axis, and condition (8) is modified to

$$\dot{I}_p\left(\frac{1}{2} + \ln\frac{r_a}{r_p}\right) > I_p \frac{\dot{r}_p}{r_p} \qquad (9)$$

This condition shows that the enhancement should be large for a high current, a high expansion velocity and/or a small plasma radius. For a stationary radius ($dr_p/dt = 0$), inequality (8) is only valid for a negative time derivative of the plasma current, in agreement with Haines's (1959) analytical solution for a rigid conductor. According to equation (9), the inverse skin effect can be observed for slightly negative or even positive dI/dt if the right-hand term is large enough.

The thermalization of the pinching plasma on axis is accompanied by a high power continuum radiation emission (Kaufmann, 1969). This radiation may be responsible for further ionization of residual gas near the plasma column. Thus, a highly conducting plasma shell can be created in

the vicinity of the central pinch column as an acting path for negative current flow (Fig. 6).

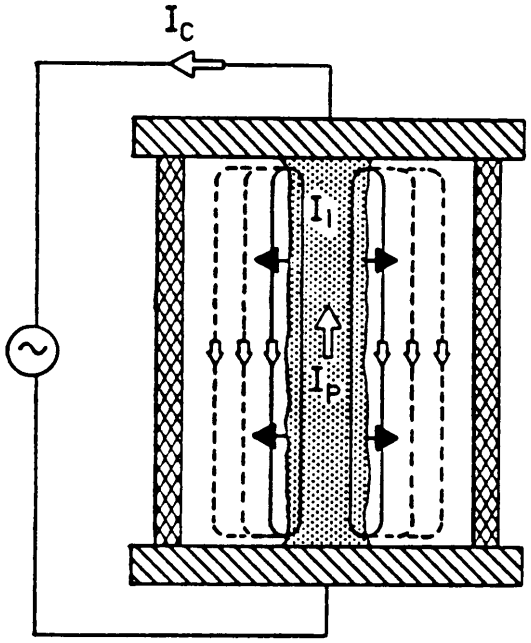

Fig. 6 - Sketch of the current distribution inside the discharge tube as a result of the inverse skin effect: $I_p = I_c + I_i$, with I_p: plasma current, I_c: circuit current, I_i = induced current.

Driven by the repulsive electromagnetic forces, this negative current layer is moving outward. The ejection happens much faster than the implosion due to less mass involved in the acceleration. Its velocity is 17 cm/μs compared to an implosion speed of 4.5 μs/cm (Fig. 2).

The ejection yields an impulsive force directed towards the axis and acts on the central column in a stabilizing manner.

6. CONCLUSIONS

The experiments demonstrated the onset of a favourable current and field enhancement due to the inverse skin effect which can almost double the pinch current.

Based on the law of flux conservation, a simple condition could be derived which is valid for a spatially and temporally changing conductor radius. The wide parameter range in which the inverse skin effect is

observed suggests that this phenomenon is also relevant for other kinds of dynamic high current plasma discharges (Butov and Matweev, 1981; Finken and Ackermann, 1982; Skowronek and Romeas, 1985).

By the inverse skin effect, magnetic field energy from the external field outside the plasma is transferred to the central pinch region. This effect proves very favourable for the application of a plasma lens, which mainly uses the central magnetic field for focusing.

An important result is also the delayed onset of instabilities due to the reacting force of the ejected current layer onto the pinch column. This stabilizing effect can be expected not only in such large scale plasmas as discussed in this paper, but also in micropinches which might be used as plasma lenses to achieve luminosity enhancement in the final focus region of colliding beam experiments.

ACKNOWLEDGEMENTS

The authors are very much indebted to Professor F. Dothan, from the Hevrew University in Jerusalem, for valuable discussions. We thank Y. Thébault and M. van Gulik, from CERN, for their technical assistance.

REFERENCES

Autin B., Riege H., Boggasch E., Frank K., De Menna L. and Miano G. (1987), IEEE Trans. Plasma Sci., PS-15, 226.

Billault P., Riege H., van Gulik M., Boggasch E., Frank K. and Seeböck R. (1987), CERN Report 87-13.

Blöss D., Kamber I., Riege H., Bittner G., Brückner V., Christiansen J., Frank K., Hartmann W., Lieser N., Schultheiss C., Seeböck R. and Steudtner W. (1983), Nucl. Instr. Methods, 205, 173.

Bötticher W. (1968), Plasma Diagnostics, Edited by W. Lochte Holtgreven (North Holland Publishing Co., Amsterdam), p. 617.

Boggasch E., Brückner V. and Riege H. (1985), Proc. of the 5th IEEE Pulsed Power Conference, Edited by P.J. Turchi and M.F. Rose (IEEE, New York), p. 820.

Boggasch E., Grüb R. (1987), Rev. Sci. Instr., 58, 1382.

Boggasch E. (1987), Die Plasmalinse, eine Stromstarke z-Pinch-Entladung zur Fokussierung geladener Teilchen in Hochenergiebeschleunigern, Dissertation, University of Erlangen.

Burkhardt L.C. and Lovberg R.H. (1958), Proc. of the 2nd International Conference on the Peaceful Uses of Atomic Energy, Geneva, Vol. 32, p. 29, United Nations.

Butov I. Ya. and Matveev Yu.V. (1981), Sov. Phys. JETP, 54, 299.

Dothan F., Riege H., Boggasch E. and Frank K. (1987), J. Appl. Phys., 53, 226.

Finken K.-H. and Ackermann U. (1982), J. Appl. Phys., 53, 226.

Forsyth E.B., Lederman L.M. and Sunderland J. (1965), IEEE Trans. Nucl. Sci., NS-12, 872.

Haines M.G. (1959), Proc. Phys. Soc., 74, 576.

Jones I.R. and Silawatshananai C. (1980), Plasma Phys., 22, 501.

Kaufmann M. (1969), Z. Phys., 225, 216.

Kvartskhava I.F., Matveev Yu.V., Khautiev E.Yu. (1971), Nucl. Fusion, 11, 349.

Skowronek M. and Romeas P. (1985), J. Appl. Phys., 57, 2519.